An Improved Rectenna Design for Battery-free Wireless Sensors and Structural Health Monitoring

Alassane Sidibe, Alexandru Takacs, Abderrahim Okba, Gael Loubet

An Improved Rectenna Design for Battery-free Wireless Sensors and Structural Health Monitoring

A. Sidibe, A. Takacs, A. Okba, G. Loubet
LAAS-CNRS, Université de Toulouse, CNRS, UPS, F-31400 Toulouse, FRANCE
asidibe@laas.fr, atakacs@laas.fr, aokba@laas.fr, gloubet@laas.fr

***Abstract*— This paper addresses the design and the characterization of an improved rectenna operating with low power density. As compact as possible, the surface of the fabricated rectenna is only 66 cm^2 that is only 0.057 of a square wavelength at the operating frequency (868 MHz). A small size (15 x 9 cm^2) reflector plane behind the rectenna increases the amount of the harvested dc power of the rectenna: the harvested dc power is greater than 100 µW (dc voltage greater than 1V) when the rectenna is illuminated with radiofrequency power densities greater than 0.78 µW/cm^2. Additionally, a comparison between different configurations of the rectenna is presented.**

Keywords*— Wireless Power Transmission; Rectenna; Energy Harvesting; Wireless Sensor

I. INTRODUCTION

Structural Health Monitoring (SHM) of buildings, public and civil infrastructures requires collecting various physical parameters (e.g. temperature, humidity, vibrations, etc.) by using wireless sensors (WS). These WS can be embedded in concrete or into the structure of the building [1]. Owing to the difficult access to these environments for maintenance, some systems necessitate the use of battery-free WS. One approach to implement battery-free WS is to use Energy Harvesting (EH) or Wireless Power Transmission (WPT) techniques. In a WPT scenario, a rectenna is typically used to harvest and convert in a dc signal, the energy of electromagnetic waves generated by a dedicated RF source. This dc energy can be used to power a battery-free WS thought the use of a power management unit and a storage element (capacitor/supercapacitor).

This paper addresses the design and characterization of improved rectennas operating in the ISM 868 MHz frequency band designed for SHM applications. As compared with the rectennas presented in [1], [2], a limited-size reflector plane, compatible with the integration constraints of the targeted applications, was added. The main goal was to improve the dc voltage and power harvested by the rectenna when illuminated with low power densities. Section II presents the topology and the design of the proposed rectenna. The obtained experimental results are discussed in Section III. This rectenna is intended to be embedded in a concrete cavity as presented in Section IV.

II. RECTENNA : TOPOLOGY AND DESIGN

The standard rectenna topology shown in Fig. 1 was adopted in this paper. It consists of a compact flat dipole antenna [2] connected with a Schottky diode (HSMS-285B) mounted in series configuration through a dedicated matching circuit.

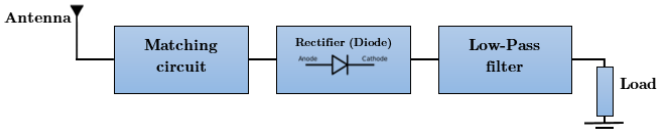

Fig. 1. Rectenna topology.

A. Rectifier circuit

The rectifier was designed and optimized to operate under low radiofrequency (RF) input power (around -15 dBm). A zero-bias Schottky diode (HSMS-285B) mounted in series configuration was selected to implement the rectifier. The matching circuit consists of a 33nH lumped inductor (Te Connectivity 36501J Series) and a short-circuited folded stub. The ADS schematic of the rectifier and its matching circuit is depicted in Fig. 2. For accurate simulation results, the inductance was modeled by a 36nH inductance according to the vendor's specification at 900MHz [4].

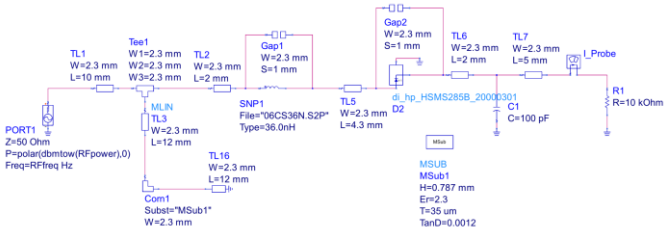

Fig. 2. Schematic model (ADS) of the rectifier and its matching circuit.

In order to have more accurate simulation results, a co-simulation technique was also adopted. The layout of the matching circuit was simulated using Momentum (methods of moment electromagnetic simulator) of ADS. As shown in Fig. 3, only the RF part for the rectifier (before the diode) was electromagnetically (EM) simulated in Momentum and then imported in ADS schematic through an EM model. A Harmonic Balance (HB) simulation method was adopted in order to model the nonlinear behavior of the Schottky diode/rectifier.

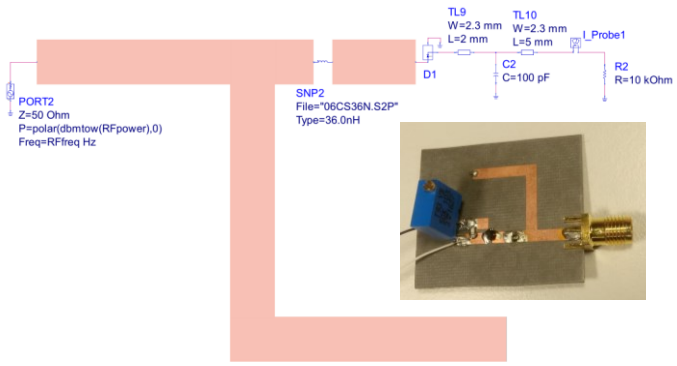

Fig. 3. Co-simulation model (Momentum/ADS) of the rectifier. The inset shows a photo of the manufactured recifier prototype.

The rectifier (Fig. 3) was prototyped on Rogers RT/Duroid 5870 substrate (substrate thickness: 0.787 mm, relative electric permittivity: 2.3 and loss tangent: 0.0012). Fig. 4 shows a comparison of the reflection coefficient between simulation (HB simulation using the ADS circuital model represented in Fig. 2, co-simulation Momentum/HB as represented in Fig. 3) and experimental results. The reflection coefficient of the Rectenna is measured between 800MHz and 1GHz using an Anritsu "37397D" vector network analyzer and a standard SOLT calibration. We observe a good correlation between measurements and simulation. The frequency shift between Momentum simulation/measurements is only 30 MHz that is 3.5 % as compared with the targeted frequency: 868 MHz.

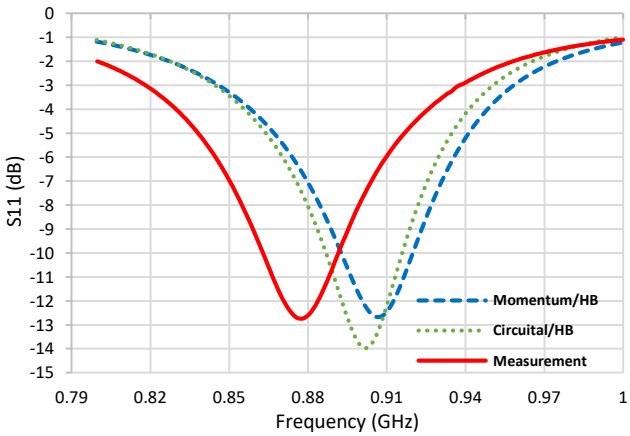

Fig. 4. Measured and simulated reflection coefficient of the rectifier for an input RF power of -15dBm.

The setup used for the rectifier's characterization is composed of a power generator "MG3694B" from Anritsu connected with the rectifier under test. The maximum measured RF to dc conversion efficiency of this rectifier is about 35% for a dc load of 10 kΩ and an input RF power of -15 dBm.

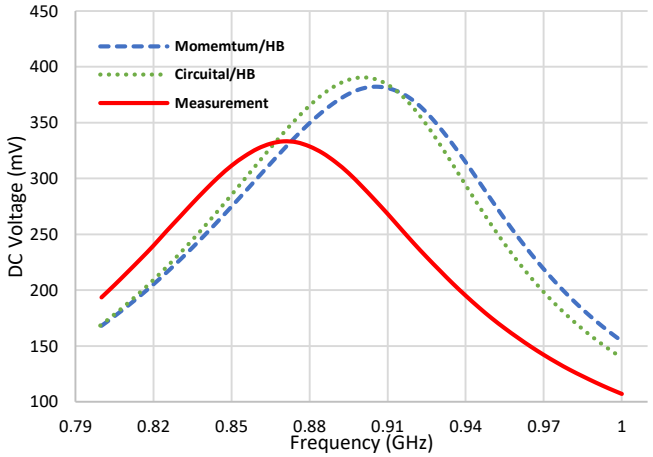

Fig. 5. DC harvested voltage for the rectifier as function of the frequency.

B. *Antenna*

For the rectenna implementation, a compact flat dipole antenna operating in the ISM 868/917MHz band was used. The dimensions, the topology and the design methodology of this antenna are reported in [2].

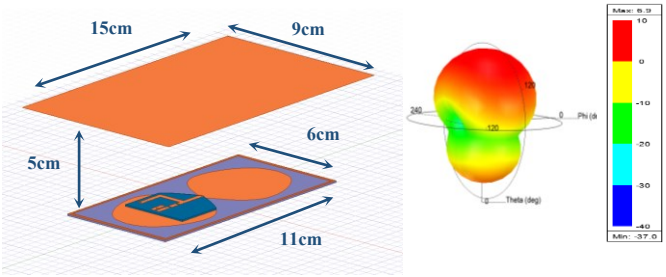

Fig. 6. HFSS antenna/rectenna simulation model (left) and the 3D simulated radiation pattern (gain in dB).

In order to increase the maximum gain of a flat dipole antenna and thus the DC power harvested by the rectenna, a reflector plate was added. The reflector size and position were chosen as a function of the integration requirement for the intended application [1]. The metallic reflector plane (RP) with finite size (15 cm x 9 cm) was positioned at 5 cm behind the antenna. We note that the position and the size of the reflector are not optimal because of the integration requirements but as illustrated in Fig. 6 the maximum gain in the upper side lobe is increased with the price of the gain reduction in the bottom side lobe. For the 2D configuration, the antenna and the rectifier were overlapped as shown in Fig. 6. The rectifier layout was taken into account in the electromagnetic simulation.

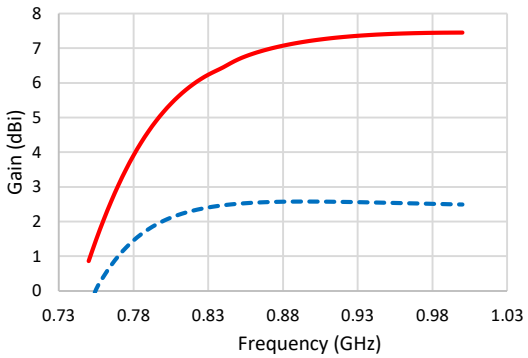

Fig. 7. Simulated antenna gain without reflector plane (continious red line) at Phi = 0° and Theta =0° and with the reflector plane (blue dash line) Phi=0° and Theta=180°.

The maximum simulated (HFSS) gain of 6.8 dBi was obtained at 868 MHz for the antenna/rectenna with reflector plane and 2.4 dBi for those without reflector plane. Therefore, we expect an increase in the harvested DC power for the rectennas with a reflector.

C. Rectenna

This section highlights the design, simulation and experimental results for the manufactured rectennas. As previously presented the antenna (compact flat dipole antenna) and the rectifier were designed, manufactured and characterized separately. The rectifier was integrated with the antenna in order to form a rectenna and then the reflector was added to increase the antenna gain and therefore the rectenna performances. Fig. 8 shows the different rectennas obtained by assembling the rectifier and the antennas (with or without reflector) namely: (i) the 3D rectenna obtained by assembling the rectifier and the antenna in a 3D manner, (ii) the 2D rectenna, in this case the rectifier overlapping the antenna surface as illustrated in Fig. 8, (iii), the 3D rectenna with its reflector plane named 3D Rectenna with Reflector Plane (3DRRP), (iv) the 2D rectenna with its reflector plane named 2D Rectenna with Reflector Plane (2DRRP).

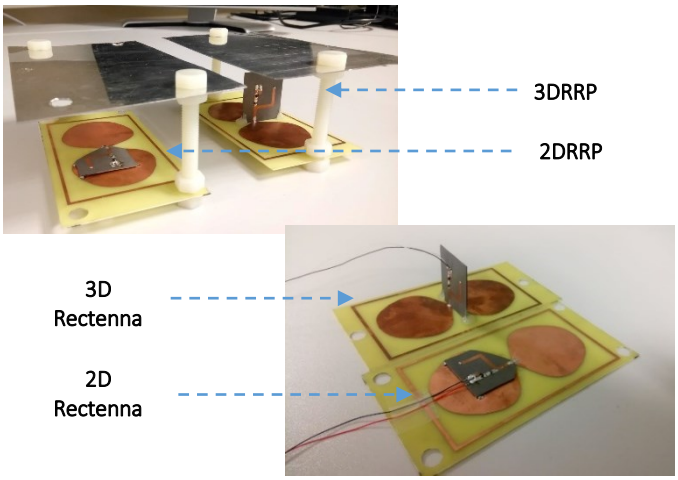

Fig. 8. Photo of the prototyped recenna: 2D rectenna without reflector, 3D rectenna without reflector, 2D rectenna with reflector plane (2DRRP) and the 3D rectenna with reflector plane (3DRRP).

2D Rectenna and 3D rectenna are similar with the compact flat dipole rectennas presented in [2]. The compact flat dipole rectennas were used as WPT interface for a LoRAWAN wireless sensor [1] but their performances were quite limited in terms of the dc power harvested for low RF power density. Thus the new designs (2D Rectenna, 2DRRP, 3D rectenna and 3DRRP) were optimized in order to increase the total amount of the harvested DC power.

As shown in Fig. 8, the antenna, the rectifier and the reflector plane (for 2DRRP and 3DRRP) are assembled together and an electromagnetic coupling may occur mainly between the antenna and the rectifier. Thus an original design and simulation approach was adopted. First, electromagnetic simulations (HFSS) were performed by taking into account the antenna (and the reflector plane for 2DRRP and 3DRRP) and a simplified PCB layout of the rectifier. Because of the electromagnetic coupling that occurs with the distributed part of the rectifier (bend stub and long microstrip lines) we separated the schematic of the rectifier (with its matching circuits) in two parts, at the level of the series inductor, as illustrated in Fig. 9. The simulated (HFSS) impedances of the antenna connected with the distributed part of the rectifier for 2DRRP and 3DRRP are depicted in Fig. 10.

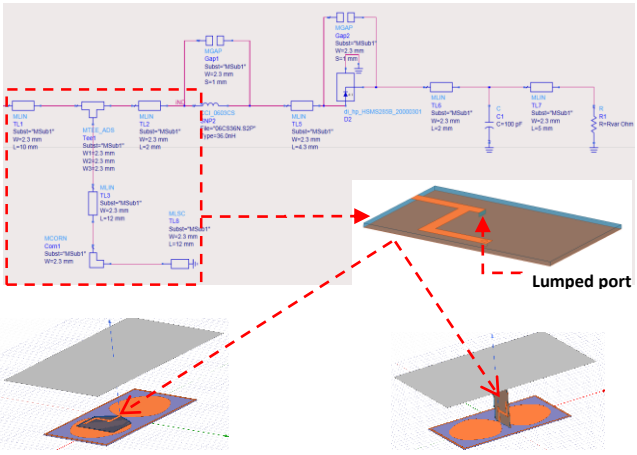

Fig. 9. PCB layout of the rectifier taken into account in HFSS simulations. A lumped port (HFSS) is used as excitation port placed at the level of the series inductor.

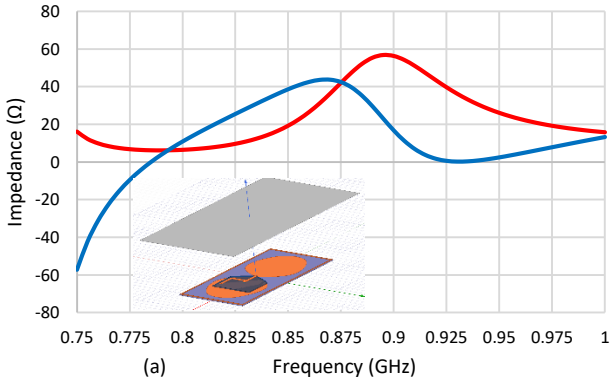

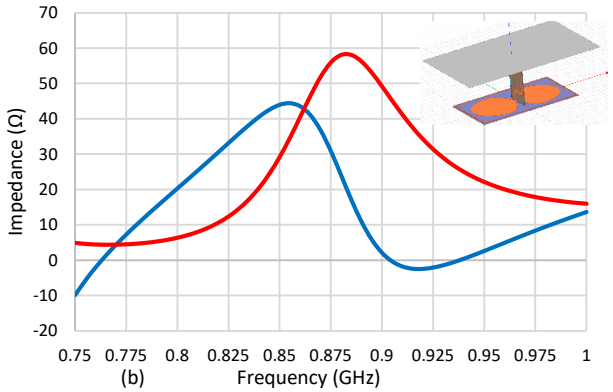

Fig. 10. Simulated (HFSS) input impedance (real part: red line, imaginary part : blue line) of the antenna on the distributed part of the rectifier for: (a) 2DRRP, (b) 3DRRP

As shown in Fig. 10, the simulated input impedance (frequency 868 MHz) of the antenna connected with the distributed part of the rectifier are: Zin = [49.7+j*38.4] Ω for 3DRRP and Zin = [34.37+j*43.69] Ω for 2DRRP. These values are inserted as port impedances in the ADS circuital model of lumped part of, as shown in Fig. 11.

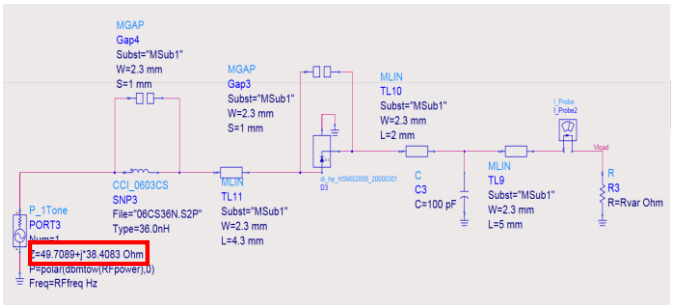

Fig. 11. Schematic model (ADS) of the rectifier with input impedance of the 3DRRP.

The RF power at the ADS harmonic balance port was estimated at 2.5dBm, which correspond roughly to an equivalent power density of 3.9 µW/cm² illuminating the rectenna. Fig. 12 depict the computed efficiency as a function of the load, for the two configurations of rectenna.

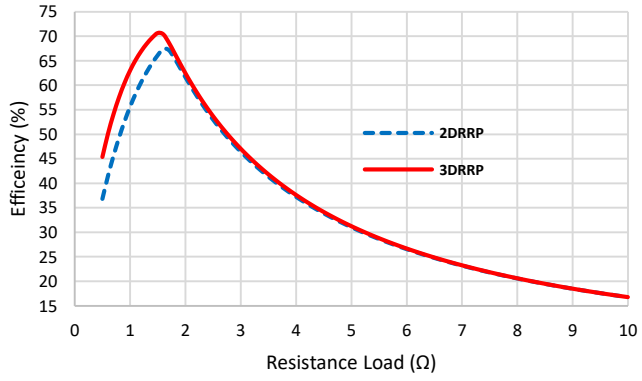

Fig. 12. Efficiency of the rectenna/rectifier (simulation results ADS) as function of the load resistance for the two configurations (2DRRP and 3DRRP) for an estimated RF power of 2.5 dBm at the input of the rectifier.

Simulation results show that the optimal load impedance is around 1.5kΩ for both Rectenna configurations. For resistance values of less than 5kΩ, 3DRRP has a higher efficiency with a maximum of 70%.

III. Experimental Results and Discussion

Four rectennas were characterized: the 2D rectenna with and without a reflector plane (2D & 2DRRP) and the 3D rectenna with and without the reflector (3D & 3DRRP). Fig. 13 shows the experimental setup used for rectenna characterization. It is composed of a signal generator connected a transmitting (Tx) patch antenna. The rectenna is connected to a digital multimeter measuring the dc voltage at the port of a resistive load. The setup is automatized by using a homemade data acquisition interface implemented in LabVIEW.

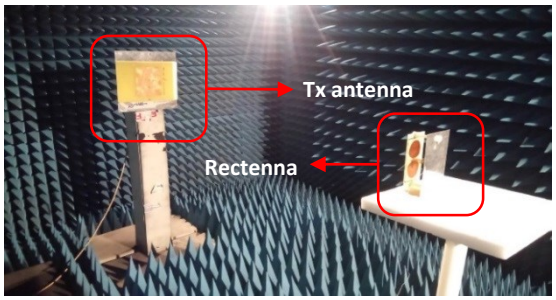

Fig. 13. Rectenna measurement setup into anechoic chamber for the 2DRRP.

The RF to dc conversion efficiency η of the rectenna is the ratio between the dc power (P_{DC}) and the corresponding power injected to the received (Rx) antenna. However, the insertion loss to the RF cable between the RF generator and the patch (about 3 dB) is subtracted from the patch gain (about 9.6 dBi). The following equations were used to compute the efficiency η and the power density of the waves illuminating the rectenna S:

$$\eta = 100\frac{P_{DC}}{P_{RF}} = \frac{4.\pi.P_{DC}}{S.G_r.\lambda^2} \quad (1)$$

$$S = \frac{E^2}{120.\pi} = \frac{P_t.G_t}{d^2.4.\pi} \quad (2)$$

where P_t is the RF power injected to the patch antenna (gain G_t) placed at the distance d (1.5m) from the rectenna under test (the antenna/rectenna gain is noted G_r).

First of all, the two different rectenna configurations (2D and 3D) without RP were characterized. The harvested dc voltage measured at the port of 10 kΩ resistive load is represented in Fig. 14. As seen in Fig. 14, the maximum measured dc voltage in function of the frequency for the 3D rectenna (1.8V) is higher than the 2D rectenna (1.6V). Note that the patch used as transmitting antenna is narrowband. Thus the harvested DC voltage decreases rapidly because of the diminution of the realized gain of the transmission patch antenna (consequently the power density generated by the RF source decreases too).

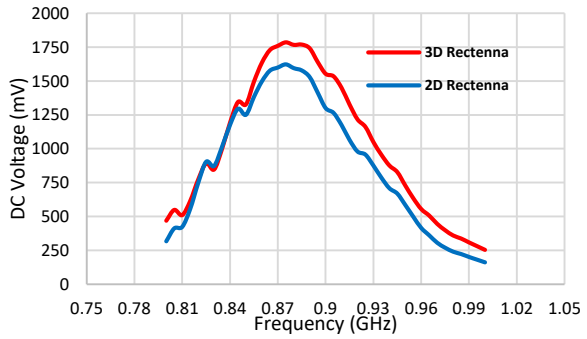

Fig. 14. Measured dc votage for rectenna without reflector plane as function of the frequency, S= {2.8 to 4.46} µW/cm², resistive load: 10kΩ.

The resulting DC power at 868 MHz and the efficiency as a function of the illuminating RF power density are presented in Fig. 15. As noted before, the 3D Rectenna is more efficient than the 2D Rectenna and reach a maximum efficiency of about 44%.

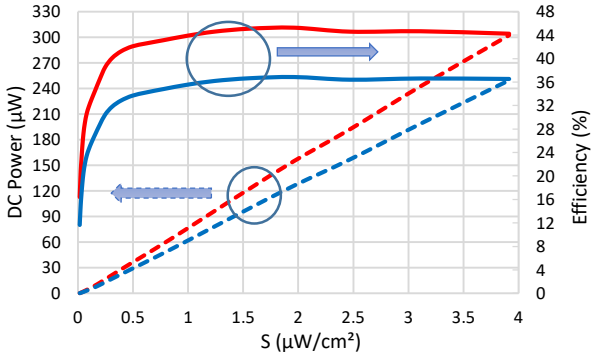

Fig. 15. Measured dc power as function of the illuminating power densities for 2D (blue line) and 3D Rectenna (red line) as function of RF power density at 868 MHz.

For further studies, 2DRRP and 3DRPP, which correspond respectively to the 2D rectenna with RP and 3D rectenna with RP, was also characterized and the obtained experimental results are depicted in Fig. 16.

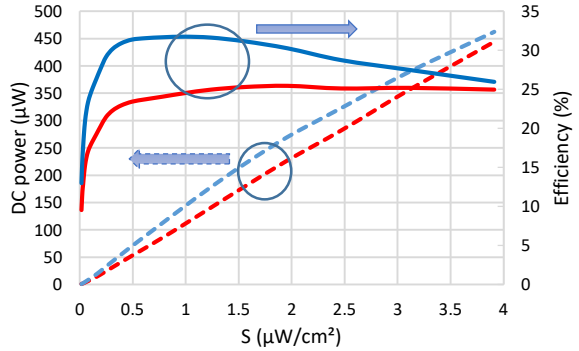

Fig. 16. Measured dc power (continuous line) and efficiency (dashed line) as function of the illuminating power densities for 2DRRP (blue line) and 3DRRP Rectenna (red line) at 868 MHz for a 10kΩ load.

The efficiency of the 2DRRP approaches a maximum of 33% at 1µW/cm² and decreases because of the unmatched impedance of the rectifier for a higher power level. As represented in Fig. 16, 2DRRP performs better while the 3D rectenna (without reflector) performs better (as represented in Fig. 15). This behavior was not expected, one possible explanation is related to the electromagnetic coupling between antenna, the rectifier and the reflector that is not well controlled/less favorable in the case of 3DRRP. A complete investigation was not yet performed (before submission).

A comparison with state of art design is given in Table I. The rectennas proposed in this paper deliver more (as compared with other rectennas operating in the same frequency band) dc power when illuminated by low values of RF power density and are valuabale candidates for implementation of a baterry-less wireless sensor (topology presented in [1]) in a concrete structure as required the ongoing research project MCBIM (Communicating Material at the disposal of the Building Information Modeling) [15]. These perspectives are discussed in the next Section.

IV. Future Works

As defined in the frame MCBIM project [15], the WS and its rectenna will be integrated inside an air cavity (maximum size 15 cm x 15 cm x 10 cm) embedded in a concrete structure as illustrated in Fig. 18. The test concrete structure was fabricated and delivered for testing in our laboratory a few days before the submission deadline. Experimentations will be performed with the rectenna embedded in concrete and more results will be presented at the conference.

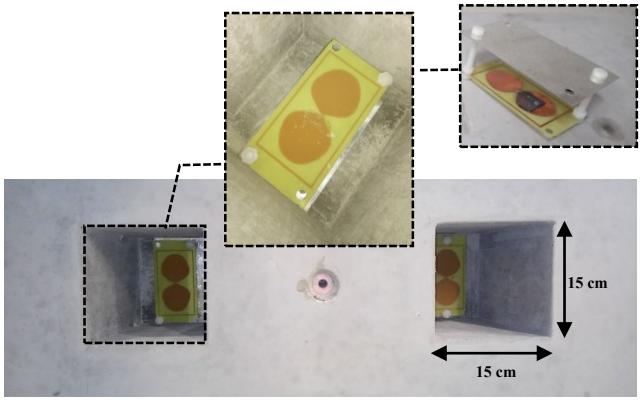

Fig. 17. 2DRRP and 3DRRP integrated inside concrete struture for SHM applications.

TABLE I. PERFORMANCES COMPARISON OF THE FABRICATED RECTENNA WITH THE OTHERS IN LITERATURE

References	Frequency (GHz)	Diode	Input Power (dBm)	Incident power density S (μW/cm²)	Efficiency (%)	Antenna gain (dBi)	Antenna size (cm x cm)	DC Power (μW)
[5]	0.868	HSMS285C	--	0.1	30.2	6.43	NR*	12.62
[6]	0.868	HSMS285B	-20	--	20	2.15	NR	2
[7]	0.9	HSMS2850	--	1	40	1.3	11 x 11 (0.11 λ^2)	47.7
[8]	0.9	MSS20-141	-15	--	30	6**	10 x 10** (0.09 λ^2)	9.5
[9]	0.915	SMS7630	-9	1	37	1.87	6 x 6 x 5.8 (0.0059 λ^3)	46.6
[10]	1.96 2.45	SMS7630 SMS7621	--	200	54.2	NR	6 x 7.5 (0.19 λ^2)	4200
[11]	2.45	HSMS2860	--	525	63	5.7	10 x 11 (0.7 λ^2)	14662.2
[12]	2.45	OMMIC ED02AH 0.20-μm GaAs	20	--	56	6.8	18 x 15 (1.8 λ^2)	56000
[13]	2.45	HSMS2852	-17.2	0.22	50%	8.6**	8 x 8.7** (0.46 λ^2)	0.09
[14]	2.45 5.8	MA4E1317	19.5 16.9	2380 8770	84.4 82.7	5 5.4	NR	75221.58 40504.71
This work								
2D				**1**	**36**	**2.64**	**11 x 6 (0.06λ^2)**	**62.84**
3D				**1**	**44**	**2.64**	**11 x 6 (0.06λ^2)**	**76.81**
3DRRP	**0.868**	**HSMS285B**	**--**	**1**	**25**	**6.8**	**15 x 9 x 5 (0.016 λ^3)**	**111.74**
2DRRP				**1**	**31.5**	**6.8**	**15 x 9 x 5 (0.016 λ^3)**	**143.77**

NR: Non reported, *: Rectenna array with large dimensions, **: Antenna with a larger reflector

V. CONCLUSION

Several rectennas designed for battery-free wireless sensors and structural health monitoring of building, public and civil infrastructures were presented in this paper. Namely the 2DRRP and 3DRRP can harvest at least 55 µW of dc power when the illuminating RF power density exceeds 0.5 µW/cm2 at 868 MHz. The next step is to introduce these rectennas into the concrete cavity in order to quantify their performances and to power a battery-free wireless sensor embedded in the concrete for SHM applications. These works are under run and more results will be presented at the conference.

REFERENCES

[1] G.Loubet, A Takacs, D. Dragomirescu, “Towards the design of wireless Communication Reinforced Concrete”, IEEE Access Special Section on Wirelessly Powered Networks: Algorithms Applications and Technologies, vol. 6, pp. 1-13,2018.

[2] A. Okba, A. Takacs and H. Aubert, “Compact Flat Dipole Rectenna for IoT Applications,” Progress in Electromagnectics Research C, vol. 87, 39-49, 2018, September 2018.

[3] G.Loubet, A Takacs, D. Dragomirescu, “Implementation of a Battery-Free Wireless Sensor for Cyber-Physical Systems dedicated to Structural Healh Monitoring Applications”, submitted on January 15, 2018 to IEEE Acess.

[4] https://www.te.com/commerce/DocumentDelivery/DDEController?Action=showdoc&DocId=Data+Sheet%7F1773163%7FE%7Fpdf%7FEnglish%7FENG_DS_1773163_E.pdf%7F1-16241

[5] S. D. Assimonis, S. N. Daskalakis, and A. Bletsas, “Sensitive and Efficient RF Harvesting Supply for Batteryless Backscatter Sensor Networks,” *IEEE Trans. Microw. Theory Techn.*, vol. 64, no. 4, pp. 1327–1338, Apr. 2016.

[6] S. D. Assimonis and A. Bletsas, “Energy harvesting with a low-cost and high efficiency rectenna for low-power input,” in 2014 IEEE Radio and Wireless Symposium (RWS), 2014, pp. 229–231.

[7] V. Palazzi, J. Hester, J. Bito, F. Alimenti, C. Kalialakis, A. Collado, P. Mezzanotte, A. Georgiadis, L. Roselli, M.M. Tentzeris, "A Novel Ultra-Lightweight Multiband Rectenna on Paper for RF Energy Harvesting in the Next Generation LTE Bands,” *IEEE Trans. Microw. Theory Techn.*, vol. 66, no. 1, pp. 366–379, Jan. 2018.

[8] V. Kuhn, C. Lahuec, F. Seguin, and C. Person, “A Multi-Band Stacked RF Energy Harvester With RF-to-dc Efficiency Up to 84%,” *IEEE Trans. Microw. Theory Techn.*, vol. 63, no. 5, pp. 1768–1778, May 2015.

[9] K. Niotaki, S. Kim, S. Jeong, A. Collado, A. Georgiadis, and M. M. Tentzeris, “A Compact Dual-Band Rectenna Using Slot-Loaded Dual Band Folded Dipole Antenna,” *IEEE Antennas Wirel. Propag. Lett.*, vol. 12, pp. 1634–1637, 2013.

[10] E. Falkenstein, M. Roberg, and Z. Popovic, “Low-Power Wireless Power Delivery,” *IEEE Trans. Microw. Theory Techn.*, vol. 60, no. 7, pp. 2277–2286, Jul. 2012.

[11] Z. Harouni, L. Cirio, L. Osman, A. Gharsallah, and O. Picon, “A Dual Circularly Polarized 2.45-GHz Rectenna for Wireless Power Transmission,” *IEEE Antennas Wirel. Propag. Lett.*, vol. 10, pp. 306–309, 2011.

[12] J. Zbitou, M. Latrach, and S. Toutain, “Hybrid rectenna and monolithic integrated zero-bias microwave rectifier,” *IEEE Trans. Microw. Theory Techn.*, vol. 54, no. 1, pp. 147–152, Jan. 2006.

[13] H. Sun, Y. x Guo, M. He, and Z. Zhong, “Design of a High-Efficiency 2.45-GHz Rectenna for Low-Input-Power Energy Harvesting,” *IEEE Antennas Wirel. Propag. Lett.*, vol. 11, pp. 929–932, 2012.

[14] Y.-H. Suh and K. Chang, “A high-efficiency dual-frequency rectenna for 2.45-and 5.8-GHz wireless power transmission,” *IEEE Trans. Microw. Theory Techn.*, vol. 50, no. 7, pp. 1784–1789, 2002.

[15] ANR-17-CE10-0014 McBIM project (Communicating Material at the disposal of the Building Information Modeling), http://www.agence-nationale-recherche.fr/en/anr-funded-project/?tx_lwmsuivibilan_pi2%5BCODE%5D=ANR-17-CE10-0014